

Supplementary Information

High-pressure synthesis of ϵ -FeOOH from β -FeOOH and its application to the water oxidation catalyst

Kazuhiko Mukai,^{*,†} Tomiko M. Suzuki,[†] Takeshi Uyama,[†] Takamasa Nonaka,[†]
Takeshi Morikawa,[†] and Ikuya Yamada[‡]

*Toyota Central Research and Development Laboratories, Inc., 41-1 Yokomichi, Nagakute,
Aichi 480-1192, Japan, and Department of Materials Science, Graduate School of
Engineering, Osaka Prefecture University, 1-2 Gakuen-cho, Sakai, Osaka 599-8570, Japan*

*E-mail: e1089@mosk.tytlabs.co.jp

Phone: +81-561-71-7698. Fax: +81-561-63-6119

^{*}To whom correspondence should be addressed

[†]Toyota Central Research and Development Laboratories, Inc., 41-1 Yokomichi, Nagakute, Aichi 480-1192, Japan

[‡]Department of Materials Science, Graduate School of Engineering, Osaka Prefecture University, 1-2 Gakuen-cho, Sakai, Osaka 599-8570, Japan

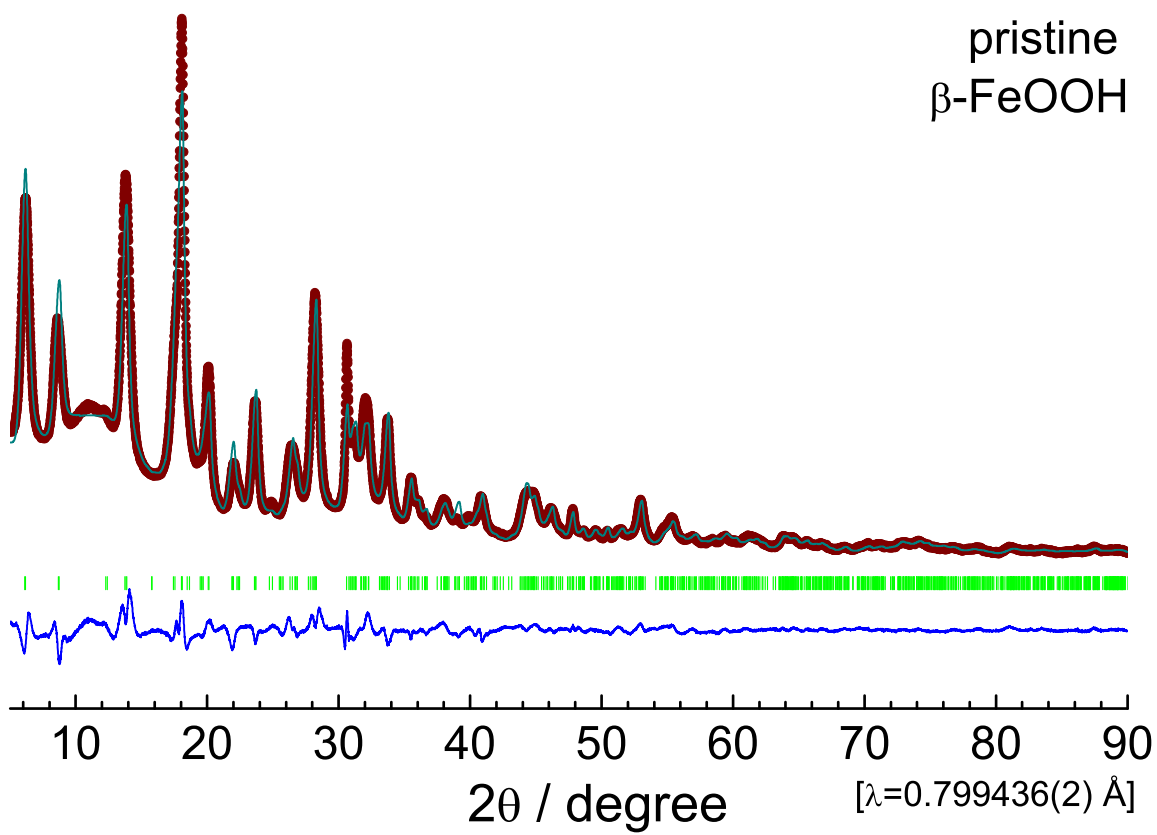


Fig. S1: Rietveld analysis result of pristine β -FeOOH. We employed the monoclinic symmetry with $I4/m$ space group by ignoring the presence of H^+ ions.

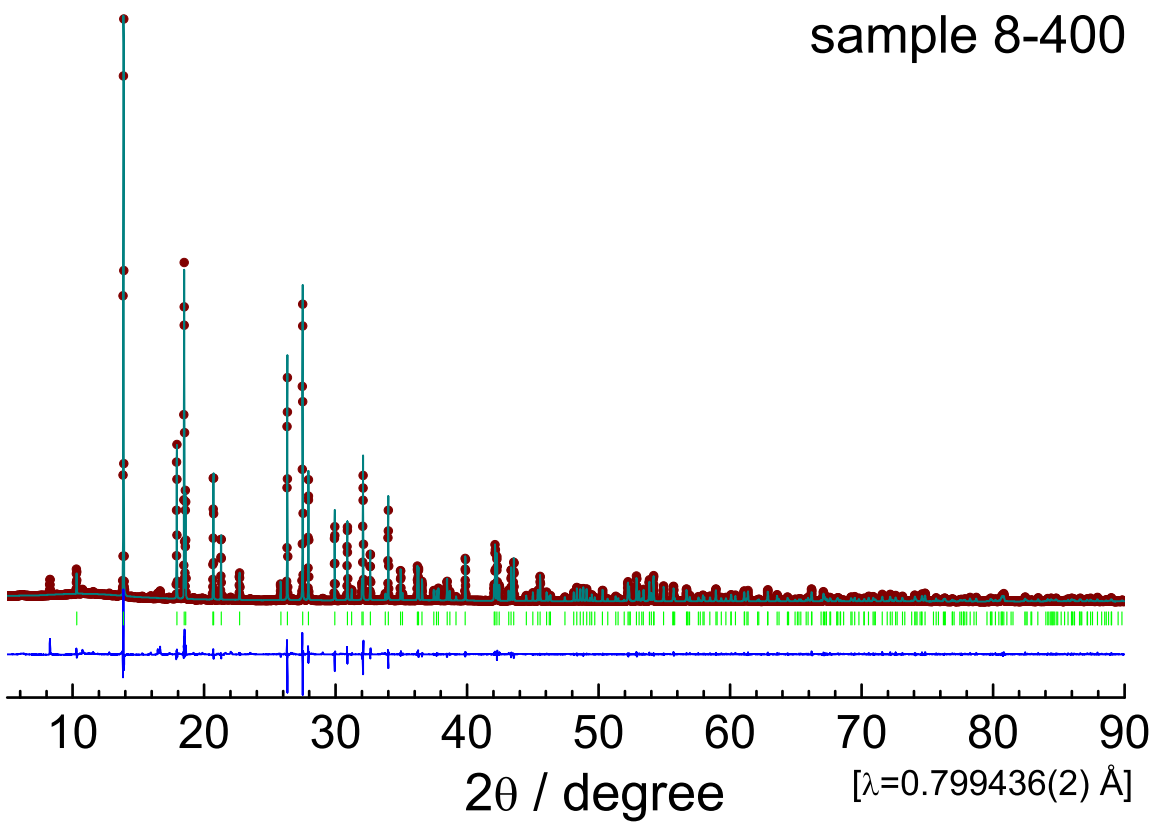


Fig. S2: Rietveld analysis result of sample 8-400, which possesses the ϵ -FeOOH-type structure with $Pmn2_1$ space group.

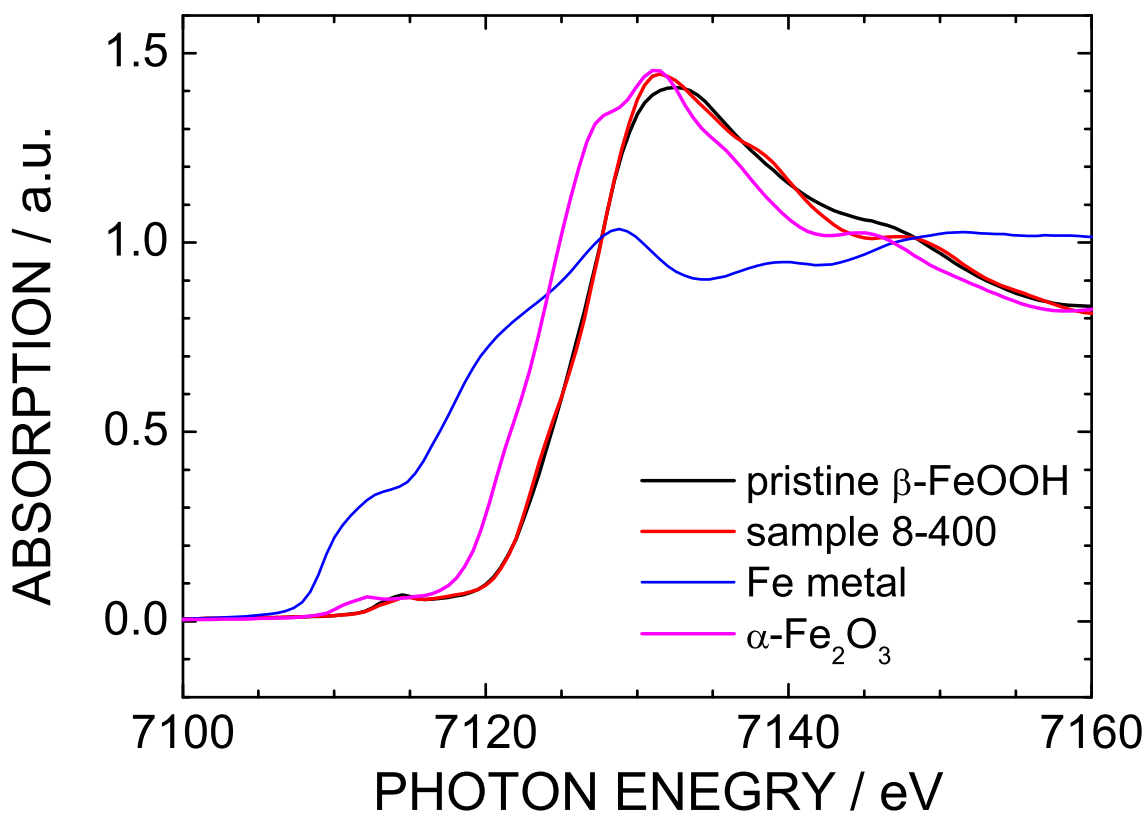


Fig. S3: Fe *K*-edge XANES spectra of Fe metal and α -Fe₂O₃ together with those of samples of pristine β -FeOOH and 8-400. The peak top energy was 7131.4 eV for α -Fe₂O₃ and 7128.7 eV for Fe metal.

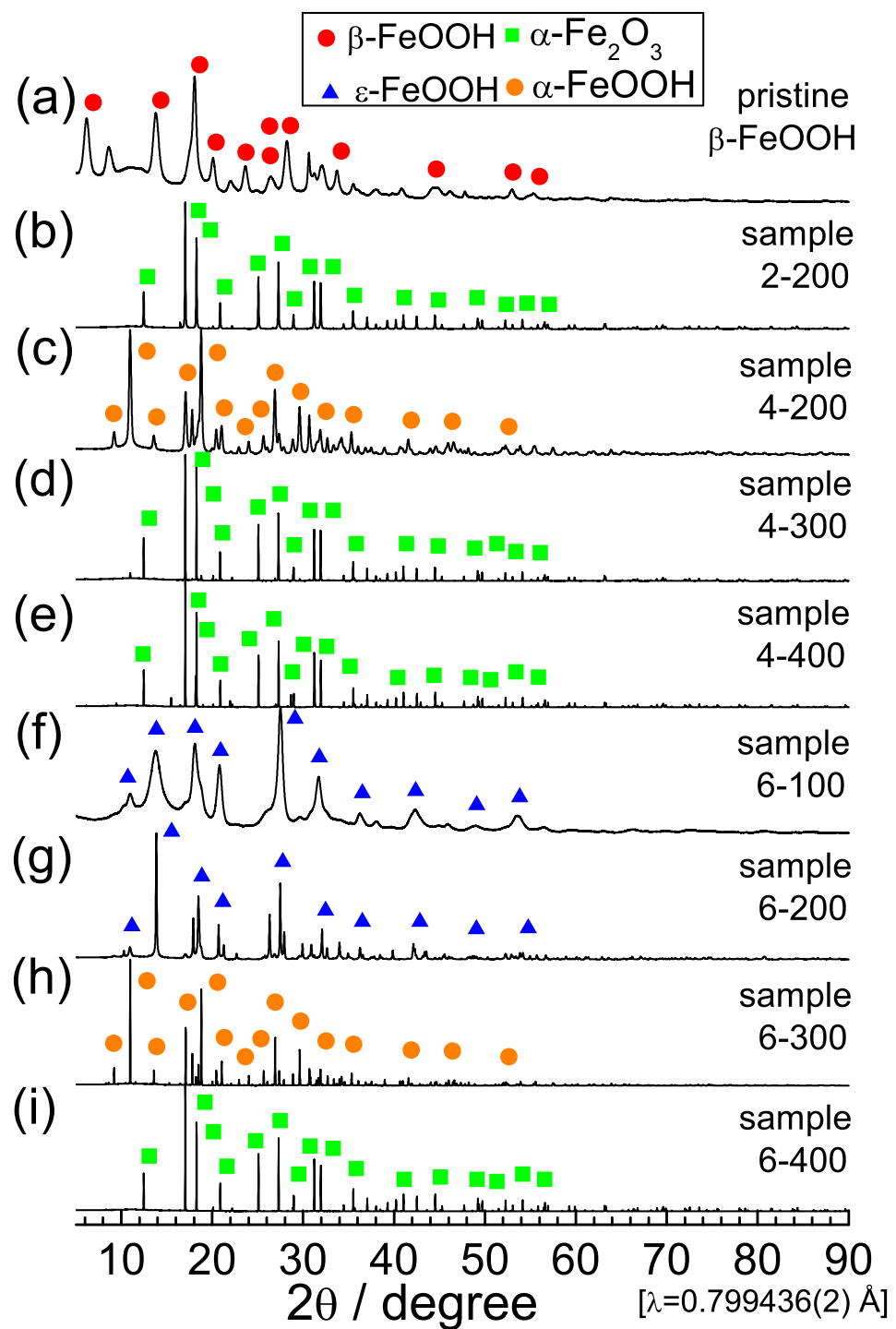


Fig. S4: Synchrotron XRD patterns of samples (a) pristine $\beta\text{-FeOOH}$, (b) 2-200, (c) 4-200, (d) 4-300, (e) 4-400, (f) 6-100, (g) 6-200, (h) 6-300, and (i) 6-400.

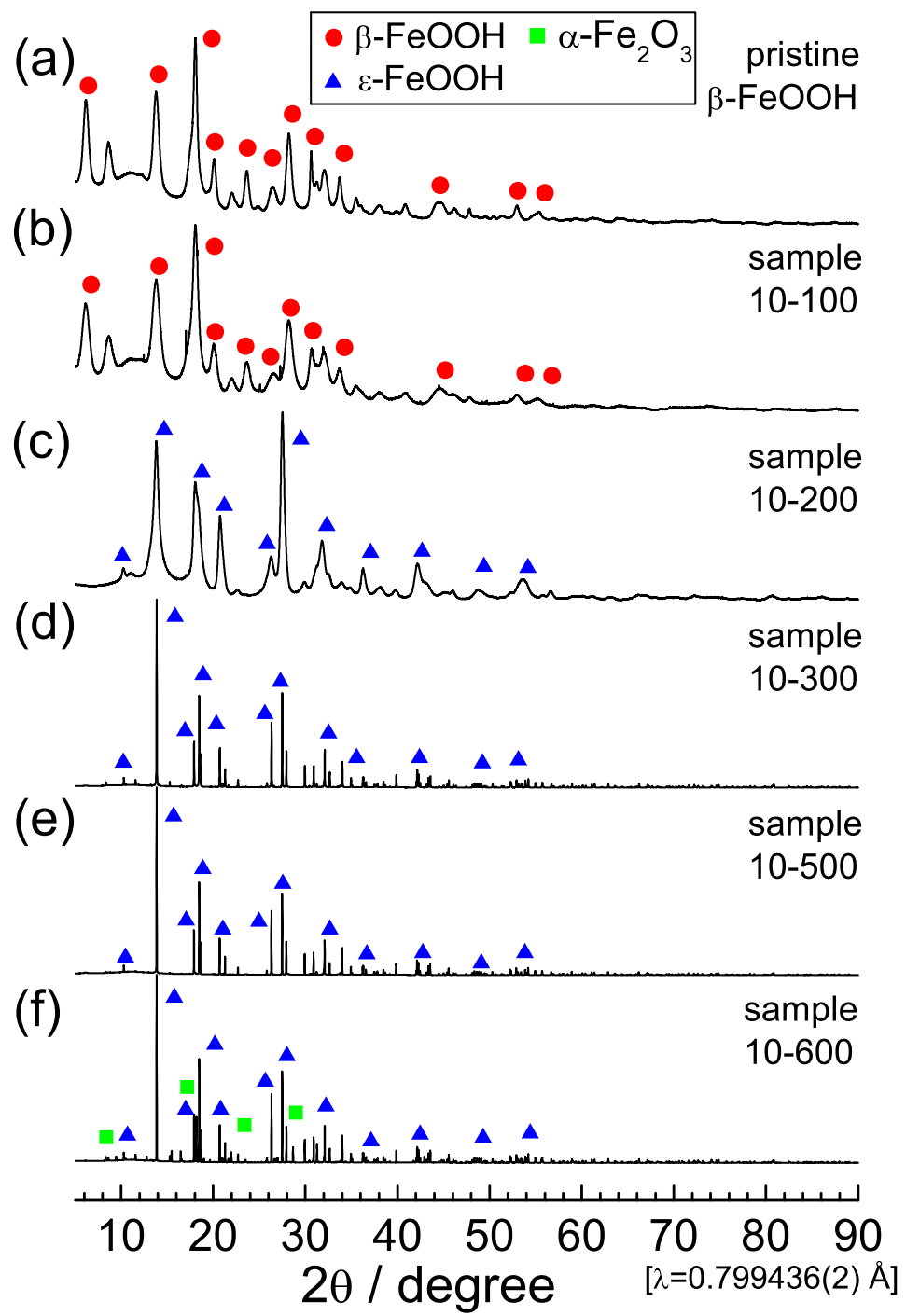


Fig. S5: Synchrotron XRD patterns of samples (a) pristine β -FeOOH, (b) 10-100, (c) 10-200, (d) 10-300, (e) 10-500, and (f) 10-600.

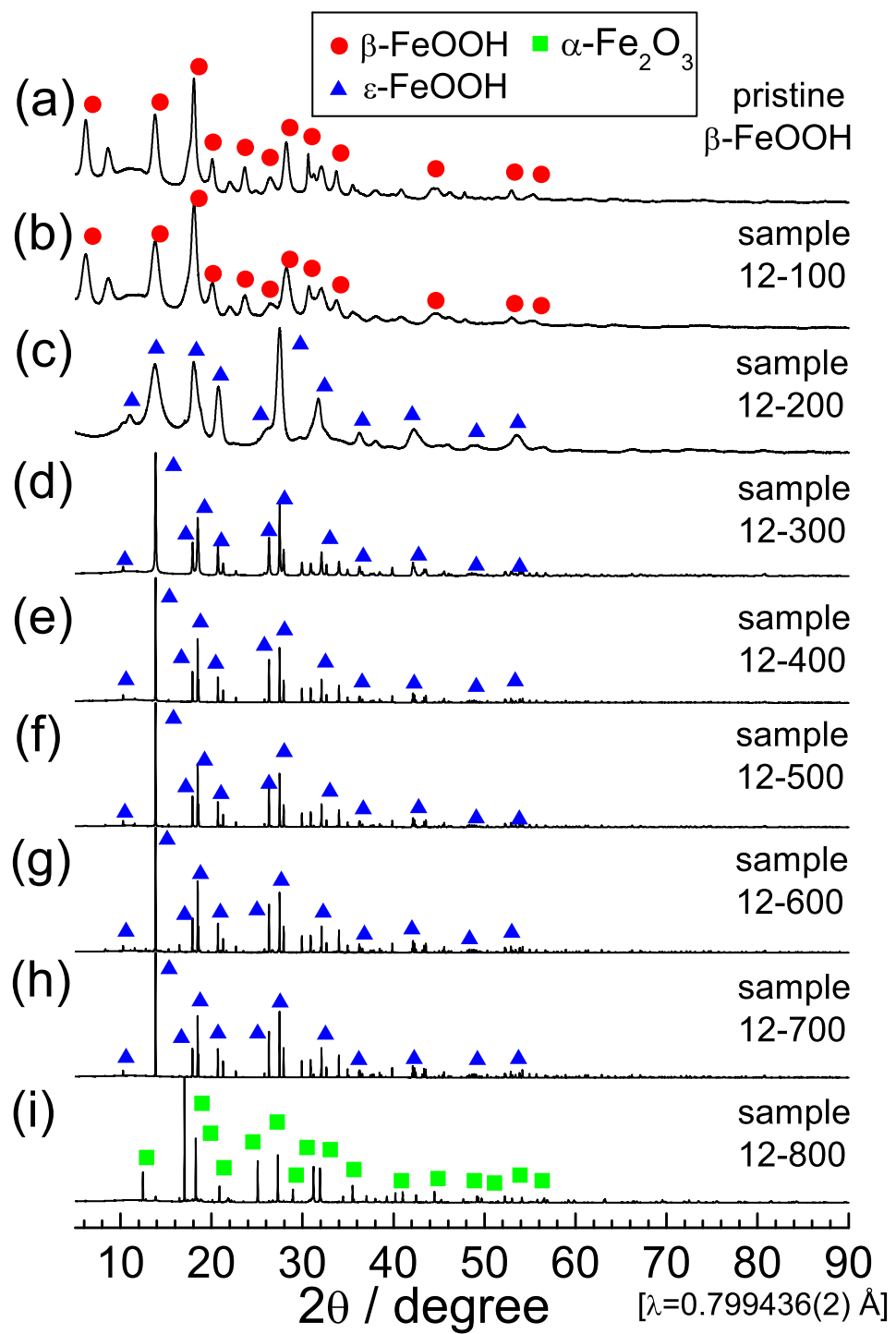


Fig. S6: Synchrotron XRD patterns of samples (a) pristine $\beta\text{-FeOOH}$, (b) 12-100, (c) 12-200, (d) 12-300, (e) 12-400, (f) 12-500, (g) 12-600, (h) 12-700, and (i) 12-800.

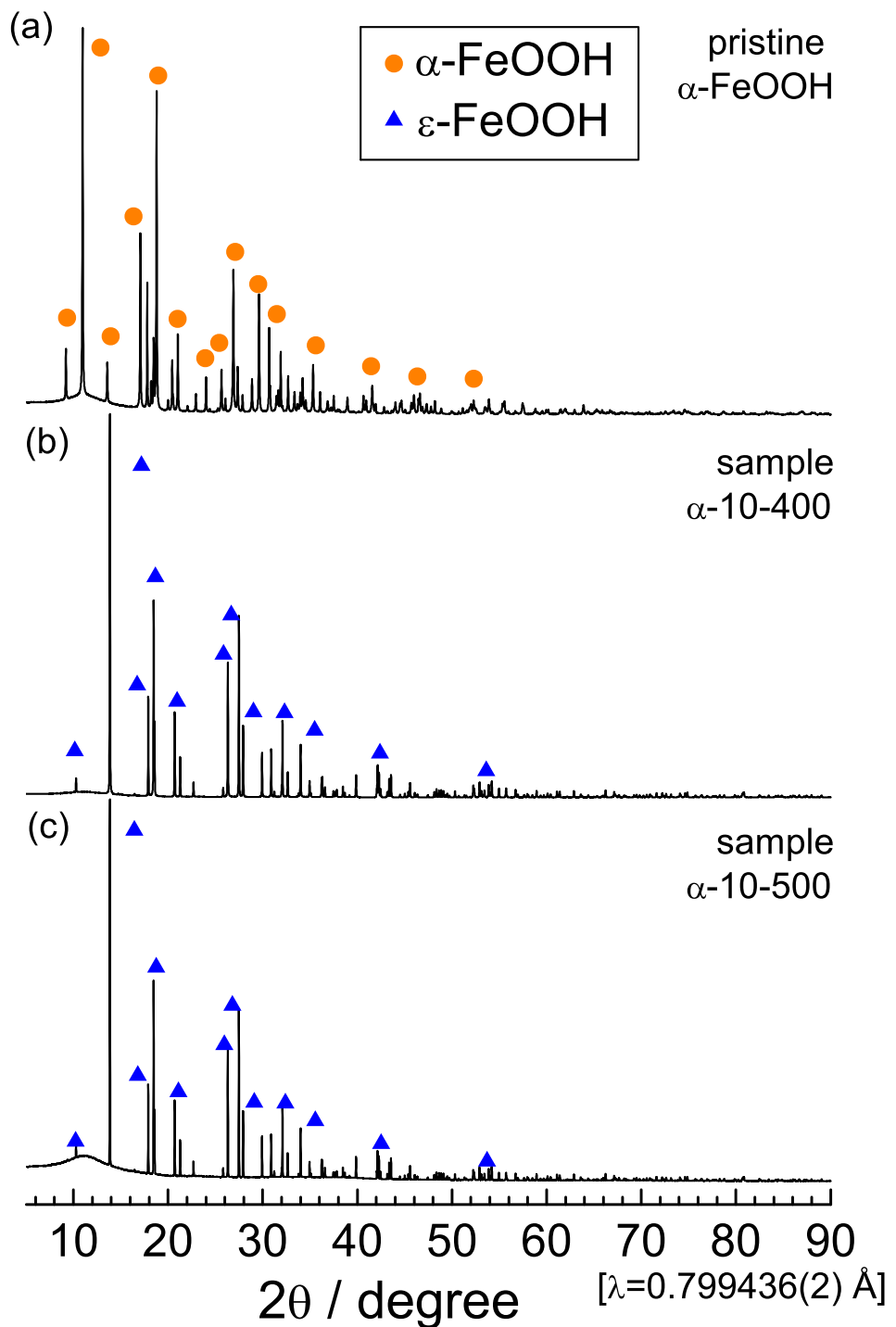


Fig. S7: Synchrotron XRD patterns of samples (a) pristine α -FeOOH, (b) α -10-400 and (c) α -10-500.

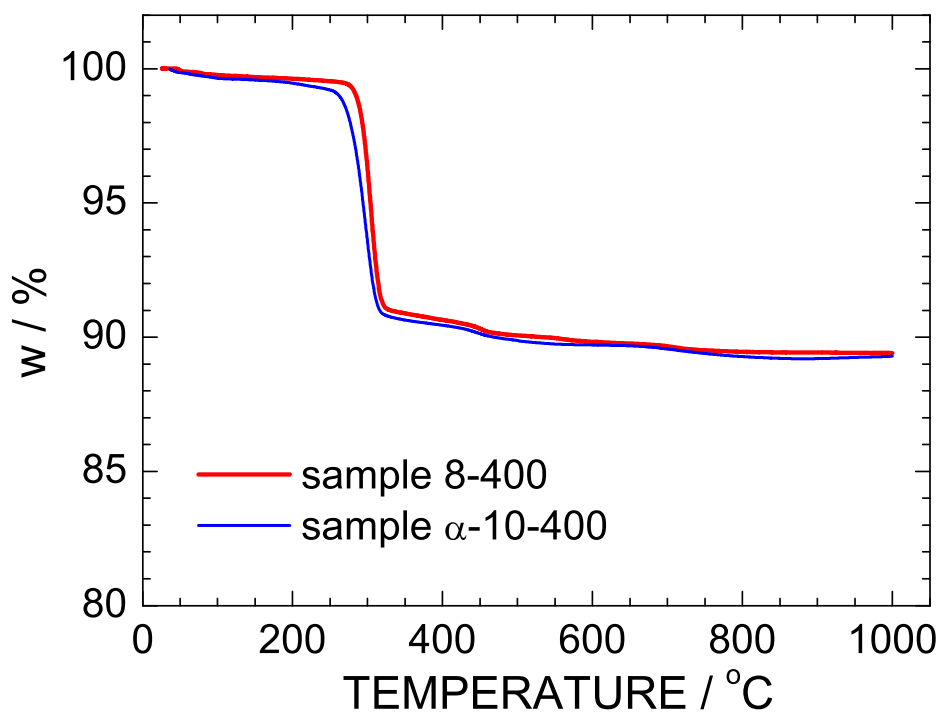


Fig. S8: Comparison of the TG curves of samples of 8-400 and α -10-400.

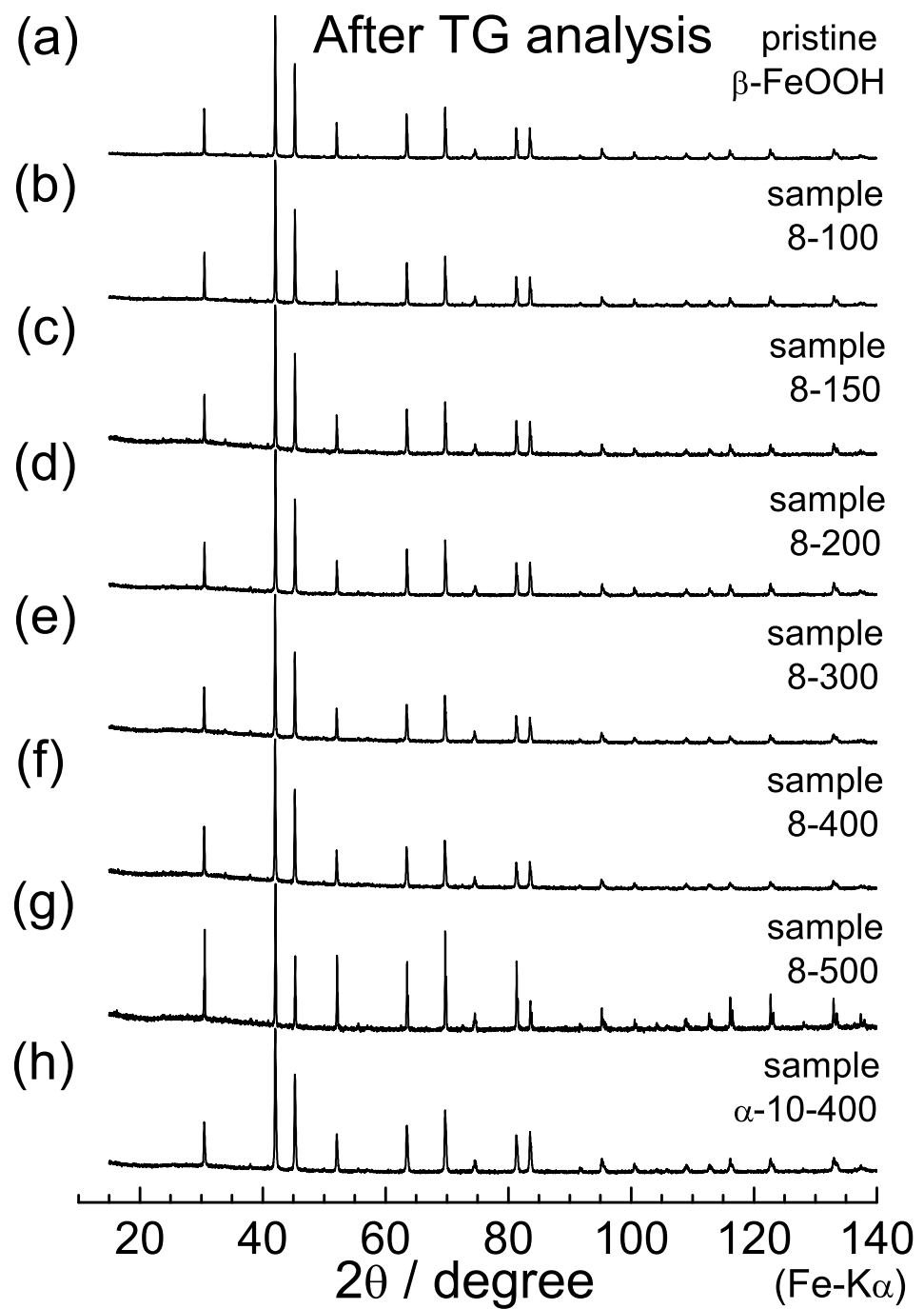


Fig. S9: XRD patterns after the TG analysis of samples (a) pristine β -FeOOH, (b) 8-100, (c) 8-150, (d) 8-200, (e) 8-300, (f) 8-400, (g) 8-500, and (h) α -10-400.

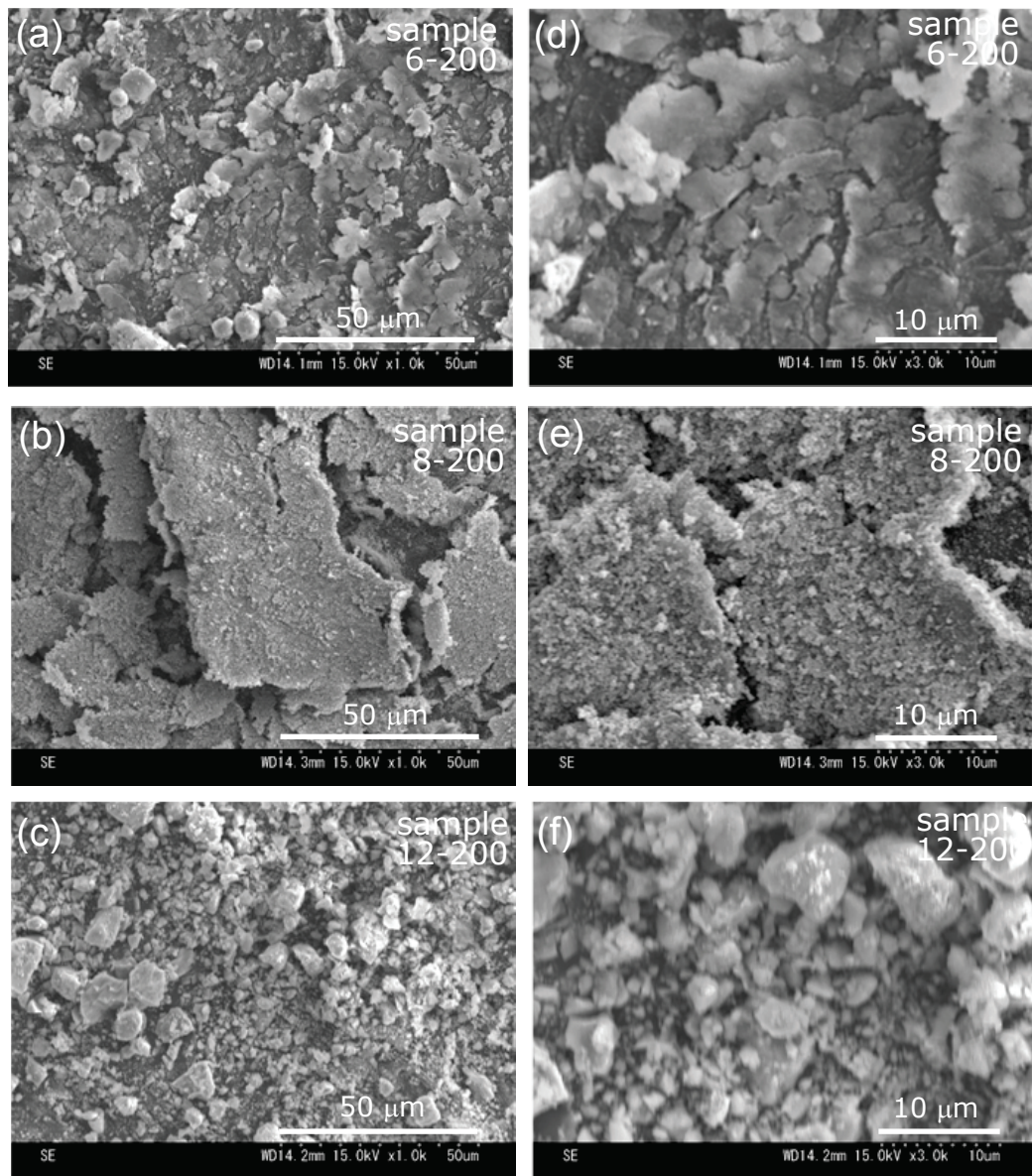


Fig. S10: SEM images at the 50 μm -scale of samples (a) 6-200, (b) 8-200, and (c) 12-200. Corresponding enlarged SEM images are shown in (d)–(f).

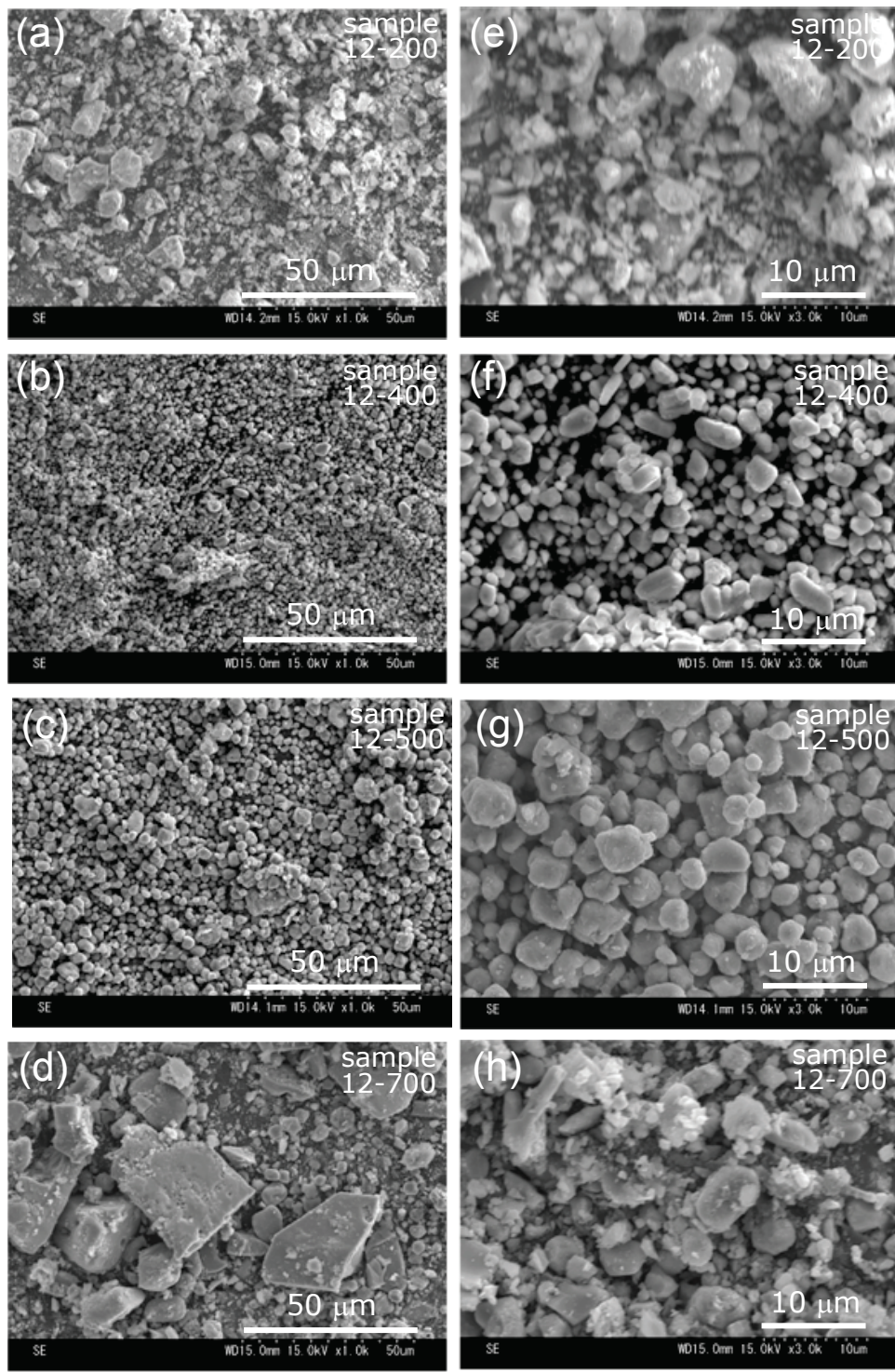


Fig. S11: SEM images at the 50μm-scale of samples (a) 12-200, (b) 12-400, (c) 12-500, and (d) 12-700. Corresponding enlarged SEM images are shown in (e)–(h).

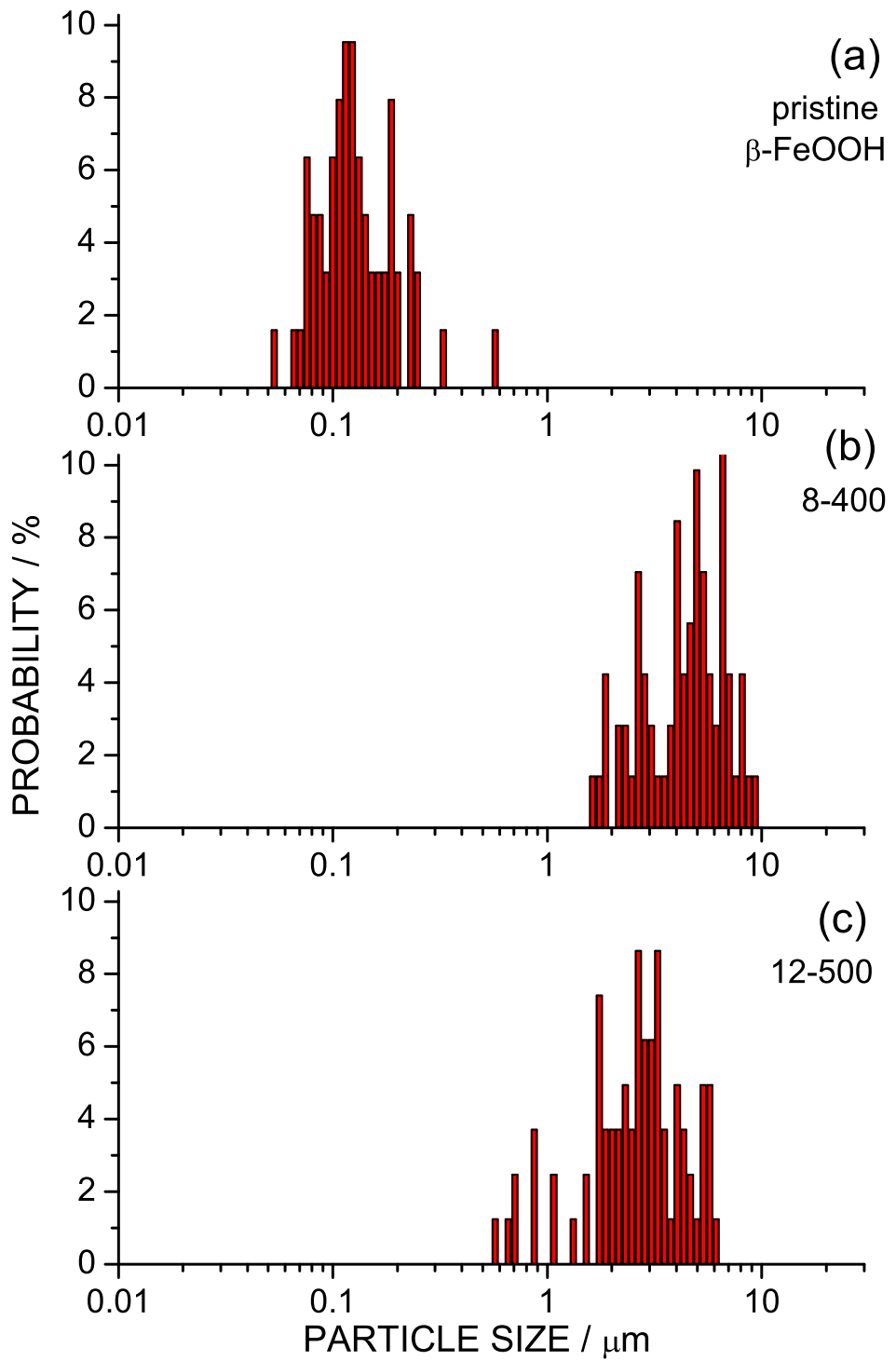


Fig. S12: Particle distribution of (a) pristine β -FeOOH, (b) 8-400, and (c) 12-500 determined by the Image J software.

Table S1: Fitting results of Cole-Cole plots for samples of pristine β -FeOOH, 8-200, 8-400, and 12-500

Sample	R_{sol} / Ω	$R_{\text{total}} / \Omega$	CPE / F	α
pristine β -FeOOH	2.66	9.42	25.7×10^{-6}	0.915
8-200	2.52	91.1	3.47×10^{-6}	0.942
8-400	2.98	5.11	3.92×10^{-6}	1.02
12-500	2.57	8.50	7.44×10^{-6}	0.953

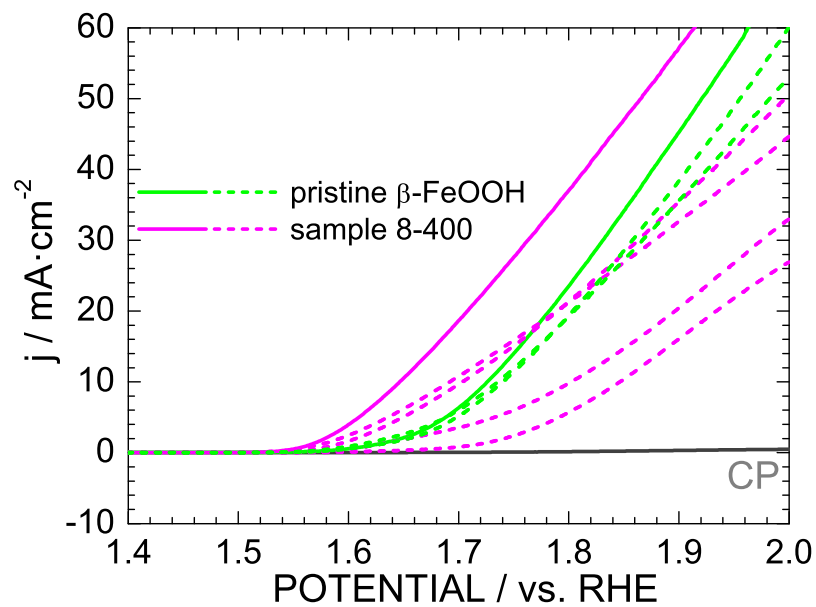


Fig. S13: Additional LSV curves of pristine β -FeOOH ans sample 8-400.

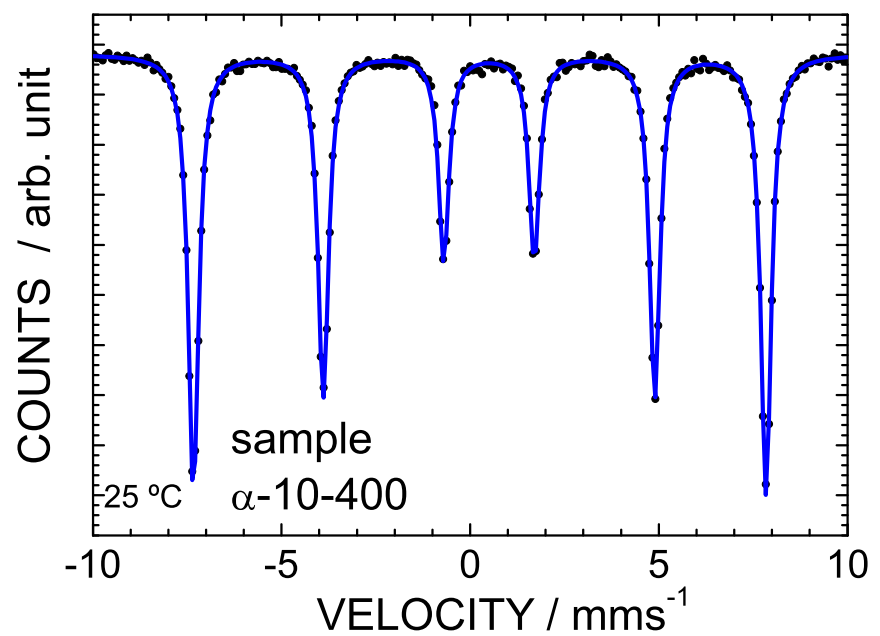


Fig. S14: Mössbauer spectrum of sample α -10-400 at ca. 25 °C.

pristine β -FeOOH

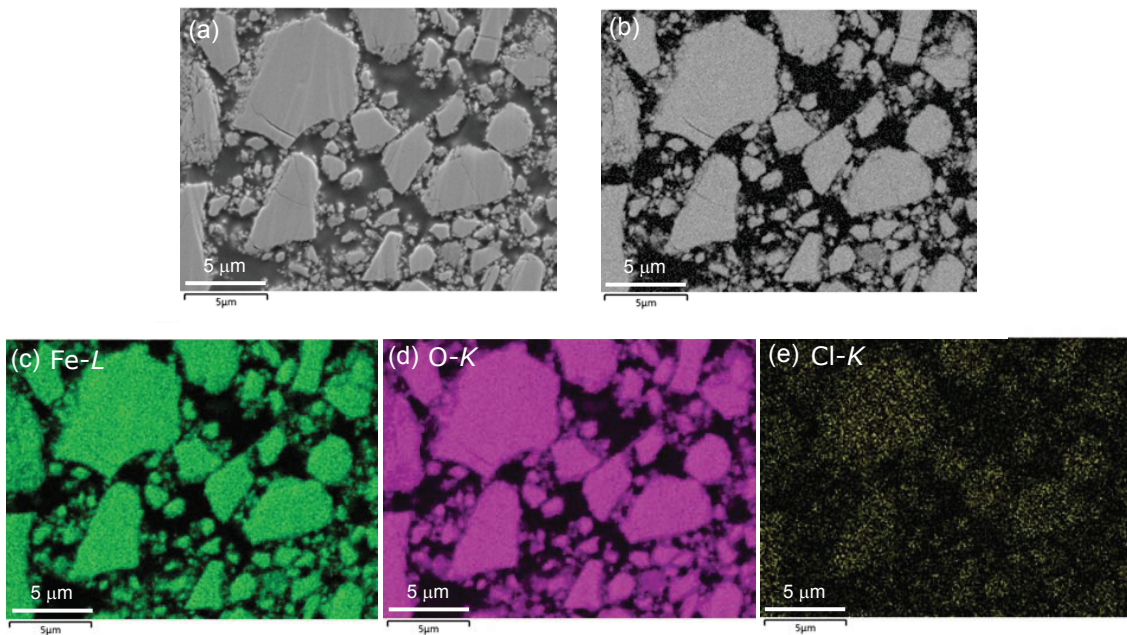
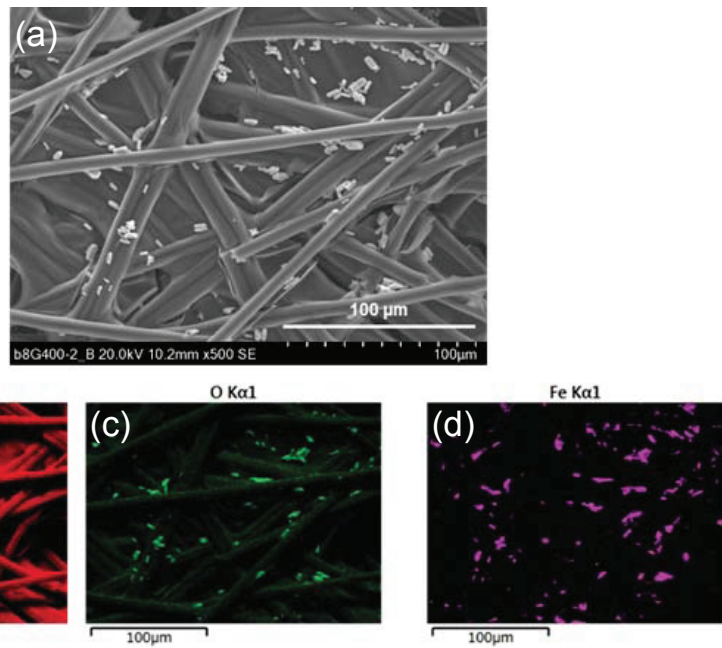


Fig. S15: SEM images of pristine β -FeOOH obtained by using (a) secondary electrons and (b) back scattered electrons. EDX mapping for (c) Fe, (d) O, and (e) Cl atoms.

Before
OER test:
8-400



After
OER test:
8-400

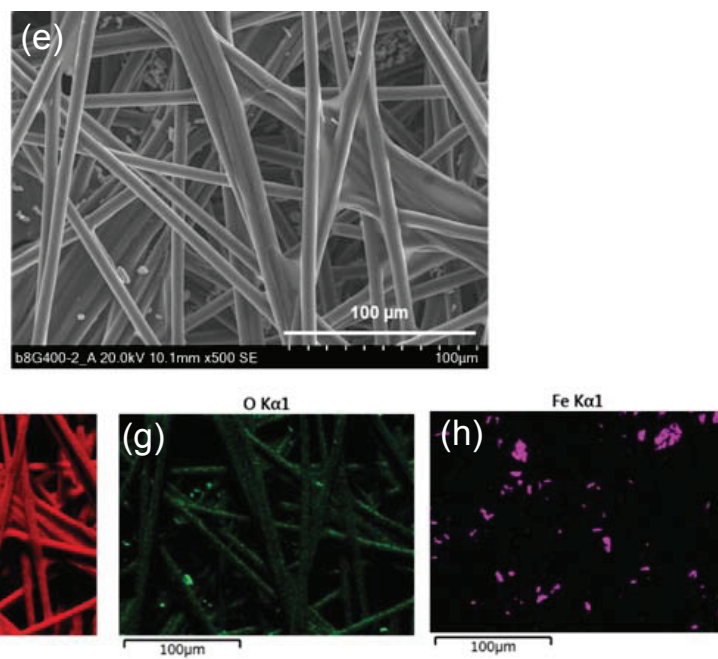


Fig. S16: SEM images and EDX mappings for sample 8-400: (a)–(d) before and (e)–(h) after.

(a) α -FeOOH($Pnma$) (b) β -FeOOH($I2/m$) (c) ϵ -FeOOH($Pmn2_1$)

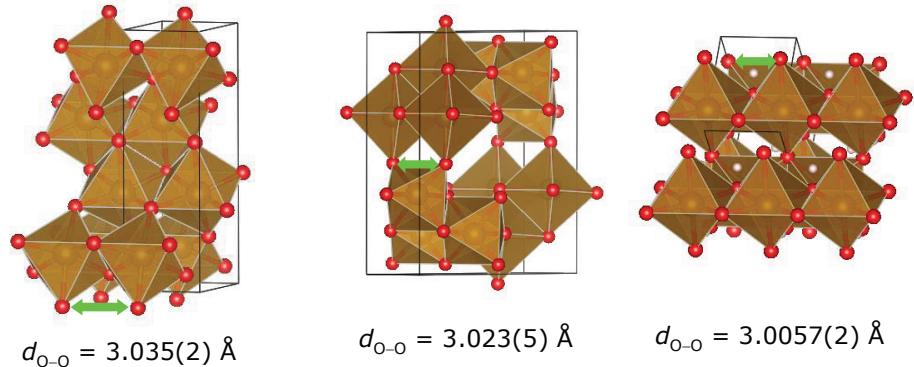


Fig. S17: Crystal structure and d_{O-O} of (a) α -FeOOH, (b) β -FeOOH, and (c) ϵ -FeOOH.